

DETAILED ANALYSIS OF SPIN-POLARIZATION OF PHOTOELECTRONS FROM 1D BI/INSB(001) SURFACE STATES

Yoshiyuki Ohtsubo^{1,2}, Jun-ichiro Kishi², Ayumi Harasawa³, Koichiro Yaji³,
Shik Shin³, Fumio Komori³, Shin-ichi Kimura^{1,2}

¹*Graduate School of Frontier Biosciences, Osaka University*

²*Department of Physics, Graduate School of Science, Osaka University*

³*The Institute for Solid State Physics, The University of Tokyo*

Electronic states with Dirac-cone (DC)-like very steep dispersion is one of the hottest topics in solid state physics in these days [1, 2]. Among them, one-dimensional (1D) or quasi-1D (Q1D) DC-like states with spin polarization, such as surface states on vicinal Bi single crystals [3] gather much attention because the backscattering in the (Q)1D states is expected to be suppressed in higher efficiency than those of 2D DCs [4]. Such feature is attractive for future application to energy-saving and high-speed spintronic devices [5].

In this work, we have studied the Q1D surface electronic structure and its spin polarization of ultrathin Bi films grown on InSb(001) substrates. About this Q1D surface state, we have already reported its DC-like steep dispersion and spin polarization [6, 7]. This year, we observed the spin-polarized structure of photoelectrons from the Q1D states on Bi/InSb(001) more in detail in order to provide further insight for the future application to spintronics. The spin polarizations of photoelectrons were observed by the spin- and angle-resolved photoelectron spectroscopy using a laser (laser-SARPES) [8] at the Institute for Solid State Physics (ISSP). The InSb(001) substrate was cleaned by the repeated cycles of Ar sputtering and annealing and the following evaporation of Bi up to ~10 atomic layers resulted in the Q1D Bi/InSb(001) surface.

Figure 1 shows the spin-resolved momentum distribution curves (MDCs) along [110] (parallel to the DC-like steep dispersion). Spin polarizations along S_x ([1-10], Fig. 1 (a), (d), (g)) shows two separate peaks with its spin polarization orientations and inverts with respect to $k_{\parallel[110]} = 0 \text{ \AA}^{-1}$. These peak positions correspond to the DC-like dispersion of the Q1D surface state observed by spin-integrated ARPES [6, 7]. These characteristics are the same in any $k_{\parallel[1-10]}$ positions (wave vectors normal to the DC-like dispersion). Moreover, the same trend is observed even above the Fermi level (E_F) at room temperature as shown in Fig. 1 (j), (k). Thanks to the thermal broadening of the Fermi distribution function, we could observe the photoelectrons from the Q1D states above E_F . The spin-polarized MDC peaks also correspond to the band dispersions observed by spin-integrated ARPES and its spin polarization orientations along S_x is the opposite to those of the states below E_F . These features are consistent with the nearly 1D surface atomic structure as well as the surface-band dispersion [6, 7].

Along the other orientations (S_y : [110] and S_z : [001]), the polarizations are almost negligible at $k_{\parallel[1-10]} = 0 \text{ \AA}^{-1}$ but become evident at the other positions. However, the polarizations along S_y does not correspond to the surface band dispersion indicated by the peak positions of MDCs with S_x spin polarizations. On the other hand, Spin polarization towards S_z becomes prominent at $k_{\parallel[1-10]} = -0.3 \text{ \AA}^{-1}$ but almost negligible at $k_{\parallel[1-10]} = +0.3 \text{ \AA}^{-1}$. These strange spin polarizations along S_y and S_z cannot be explained solely from the spin polarization of the initial states and it would be due to the photoexcitation process, so-called final-state effect. Recently, some reports were published telling that the spin polarization of photoelectrons from surface states strongly depends on the polarization (in other words, parity) of the incident photons [9, 10]. As shown in Fig. 1 (l), we changed the polar angle of the substrate for different $k_{\parallel[1-10]}$ points. So, the in-plane (out-of-plane) component of the electric field of the incident photons becomes dominant for positive (negative) wavenumbers. The drastic change of the S_z spins might be due to these different incident electric field.

In summary, we have studied the spin polarization texture of the photoelectrons from the Q1D surface states on Bi/InSb(001) in detail by using laser-SARPES. The spin-polarization structure along S_x indicated the Q1D spin-polarized structure along the steep DC-like dispersion of the surface states. The spin polarizations along the other directions (S_y and S_z) were sensitive to the photoemission experimental geometries, suggesting that the spin polarizations along these orientations are due to the photoemission final-state effect.

These results were summarized together with the results obtained last year and have been already submitted [7].

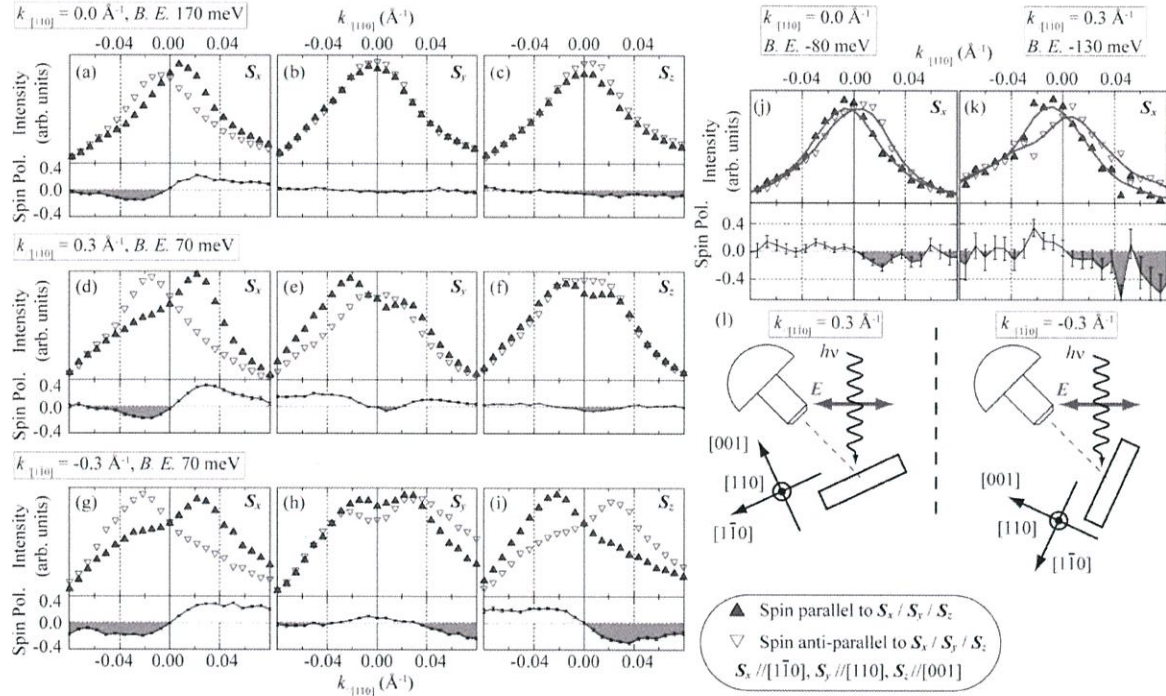


Figure 1: Spin-resolved momentum distribution curves (MDCs) along the DC-like steep dispersion ([110]) of the Bi/InSb(001) surface state at room temperature with a linearly polarized laser ($h\nu = 6.994$ eV). Binding energies and the wave vectors normal to the DC-dispersion ([1-10]) are shown. Solid curves in (j) and (k) are smoothed curves of MDCs provided as visual guides. (l) Schematics of the laser-SARPES experimental geometries.

REFERENCES

- [1] A. K. Geim and K. S. Novoselov, *Nature Mat.* **6**, 183 (2007).
- [2] M. Z. Hasan and C. L. Kane, *Rev. Mod. Phys.* **82**, 3045 (2010).
- [3] J. W. Wells *et al.*, *Phys. Rev. Lett.* **102**, 096802 (2009).
- [4] G. Autès *et al.*, *Nature Mat.* **15**, 154 (2016).
- [5] A. Manchon *et al.*, *Nature Mat.* **14**, 871 (2015).
- [6] “Spin polarization of 1D surface state on Bi/InSb(001)” J. Kishi *et al.*, Activity Report of Synchrotron Radiation Laboratory 2015
- [7] J. Kishi *et al.*, *submitted*. (arXiv: 1704.05258 (2017)).
- [8] K. Yaji *et al.*, *Rev. Sci. Instrum.* **87**, 053111 (2016).
- [9] C. Jozwiak *et al.*, *Nature Phys.* **9**, 293 (2013).
- [10] K. Yaji *et al.*, *Nature Commun.* **8**, 14588 (2017).

OBSERVATION OF INTRINSIC ELECTRONIC STATES OF HALF-METALLIC FERROMAGNETS STUDIED BY BULK-SENSITIVE HIGH-RESOLUTION SPIN-RESOLVED PHOTOEMISSION SPECTROSCOPY

Hirokazu Fujiwara,¹ K. Terashima,² M. Sunagawa,¹ T. Nagayama,¹ K. Yaji,³ A. Harasawa,³ K. Kuroda,³ T. Wakita,² Y. Muraoka,^{1,2} and T. Yokoya^{1,2}

¹*Graduate School of Natural Science and Technology, Okayama University, Okayama 700-8530, Japan*

²*Research Institute for Interdisciplinary Science, Okayama University, Okayama 700-8530, Japan*

³*Institute for Solid State Physics, University of Tokyo, Kashiwa, Chiba 277-8581, Japan*

Half-metallic ferromagnet is a key material for spintronics devices because of its 100 % spin polarization of the density of states (DOS) at the Fermi level (E_F).^[1] Chromium dioxide, CrO_2 , has the highest spin polarization obtained by point-contact Andreev reflection measurements at low temperature.^[2] However, magnetoresistance studies using magnetic tunneling junctions reported that the spin polarization exponentially decreases with increasing temperature and, as a result, CrO_2 behaves as ‘normal’ ferromagnetic metal above 50–100 K.^[3,4] The magnitude of the spin depolarization is much greater than that of magnetization measured by SQUID.^[5] As one of the reasons of the precipitous depolarization, it is suggested that an electron-magnon interaction broadens bandwidth of minority spin states above E_F and the tail of the minority spin states comes across E_F , which can permit spin-flip scattering of the conducting majority spin electrons.^[6] The minority spin state appearing at E_F by the electron-magnon interaction is so-called *non-quasiparticle* (NQP). Although the indication of existence of the NQP states have been suggested in several tunneling magnetoresistance studies,^[7] there is no direct evidence for the NQP in half-metallic ferromagnets at present. In this study, in order to demonstrate the existence of the NQP states, we performed high-resolution spin-resolved photoemission spectroscopy (SRPES) on CrO_2 films.

CrO_2 (100) epitaxial films ($T_C \sim 390$ K) grown on rutile-type TiO_2 (100) substrates were prepared by a chemical vapor deposition method.^[5] The CrO_2 films were removed from the quartz tube and then immediately placed under high vacuum for the spin-resolved PES measurements. All of the spin-resolved PES data were acquired by the laser-based spin- and angle-resolved photoemission spectroscopy (ARPES) apparatus at the Institute for Solid State Physics at the University of Tokyo. The photon energy and energy resolution were 6.994 eV and 30 meV, respectively. We magnetized the samples along the magnetic easy axis ([001] direction) by bringing the samples close to a magnet at room temperature.

Figure 1 (a) shows temperature dependence of the obtained spin polarization. At 10 K, we observed 100 % spin polarization near E_F , showing the half-metallicity of the CrO_2 film. The spin polarization decreases toward higher binding energy, which reflects the secondary electron-like background of the minority spin state as shown in Fig. 1(b).

With increasing temperature, we observed depolarization which makes the spectral shape between 500 meV binding energy and E_F more parallel to the horizontal axis, as seen in Fig. 1 (a). The energy dependence of spin polarization at 300 K fits nicely with that obtained by measurements using Xe I light ($h\nu = 8.44$ eV).^[9] From analogy with the previous study using Xe I light, the temperature-dependent depolarization arises in the whole spin-polarized energy range to decrease the macroscopic magnetization.

Finally, we mention an indication of depolarization just at E_F . In Fig. 1 (a), we find tendency that spin polarization drops from a binding energy of several 10 meV toward E_F

above 120 K. The temperature dependence of the spin polarization at E_F shows precipitous decrease with increasing temperature, as shown in Fig. 1 (c). This kind of depolarization can be a possible reason for the rapid reduction of the magnetoresistance incomprehensible from the temperature dependence of the magnetization. The energy scale of the depolarization is consistent with that of the NQP state,[6] indicating that one of origin of the depolarization is appearance of the NQP state at and above E_F .

In summary, we have performed high-resolution SRPES on CrO_2 films and observed two energy scales of the temperature-dependent depolarization, which may shed light on the characteristic many-body interaction in half-metals.

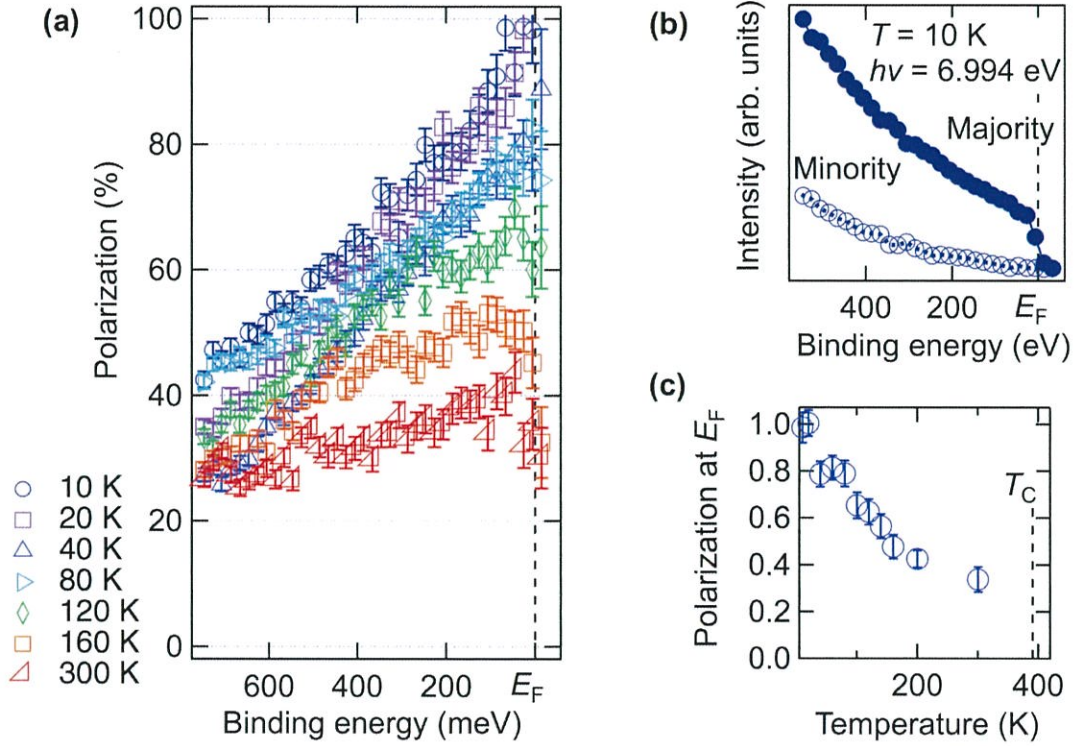


Figure 1 (a) Temperature dependence of the spin polarization as a function of binding energy of CrO_2 . The statistical error bars are estimated from $1/(S_{\text{eff}}I_{\text{total}}^{1/2})$. (b) SRPES spectrum measured at 10 K. Filled and empty circles correspond to the majority and minority spin, respectively. (c) Temperature dependence of spin polarization at E_F . Each value represents the average values in the region between 20 meV and E_F .

REFERENCES

- [1] R. A. de Groot *et al.*, Phys. Rev. Lett. **50**, 2024 (1983).
- [2] R. J. Soulen Jr. *et al.*, Science **282**, 85 (1998).
- [3] J. M. D. Coey *et al.*, Phys. Rev. Lett. **80**, 3815 (1998).
- [4] S. M. Watts *et al.*, Phys. Rev. B **61**, 9621 (2000).
- [5] K. Iwai *et al.*, J. Appl. Phys. **108**, 043916 (2010).
- [6] L. Chioncel *et al.*, Phys. Rev. B **75**, 140406(R) (2007).
- [7] L. Chioncel *et al.*, Phys. Rev. Lett. **100**, 086402 (2008).
- [8] R. Cheng *et al.*, Appl. Phys. Lett. **79**, 3122 (2001).
- [9] H. Fujiwara *et al.*, Appl. Phys. Lett. **106**, 202404 (2015).

SPIN-RESOLVED ARPES ON THE GREY ARSENIC SURFACE

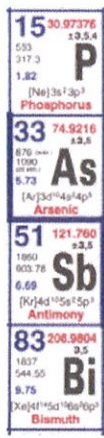
Y. Ishida, P. Zhang, K. Yaji, S. Shin

LASOR, The Institute for Solid State Physics (ISSP), The University of Tokyo

In 2008, it was experimentally established [1] that non-magnetic insulators can be classified into two categories; namely, into a topologically trivial insulator and a topologically non-trivial insulator. The classification owes to the fact that a topological number Z_2 can be assigned to each of the insulators. Z_2 takes the number of either 0 or 1 depending on the structure of the electronic bands of bulk. The insulators endowed with the non-trivial $Z_2 = 1$ exhibit novelty on their surface: The surface of a topological insulator (TI) inevitably harbours spin-polarized metallic states that show Dirac-conical dispersions. Thus, detection of the novel surface states by using angle-resolved photoemission spectroscopy (ARPES) methods has become the standard in judging the topological nature of the insulators.

Pnictogens are the chemical elements in group 15 of the periodic table. Elemental crystals of pnictogens form into semimetals, and their topological classification has been undertaken by several research groups; see Table 1: Black phosphorus is said to be topologically trivial [2]; antimony is categorized as a TI [3]; and bismuth may be topologically non-trivial, as claimed by some groups recently [4]. Meanwhile, grey arsenic remained untouched, presumably because of the obsession that arsenic is toxic. Once crystallized, however, grey arsenic itself is not poisonous unless it is heated up to temperatures above 130°C in air.

Table 1: Topological classification of the pnictogen elemental semimetals.

15/VB	Elemental semimetals	Classification
	<p>— Black phosphorus</p> <p>— Grey arsenic</p> <p>— Antimony</p> <p>— Bismuth</p>	<p>Trivial insulator Science 349, 723 (2015)</p> <p>Topological insulator PRL 118, 046802 (2017)</p> <p>Topological insulator Science 323, 919 (2009)</p> <p>Topological insulator NJP 15, 033041 (2013) PRL 117, 236402 (2016)</p>

Spin-resolved ARPES (SARPES) can directly assess the spin polarization of the bands: Thus, the technique is routinely adopted for the topological classification of the non-magnetic insulators. The laser-SARPES apparatus developed at ISSP [5] realizes the highest energy resolution of 1.3 meV and achieves a high throughput, thanks to the combination of the bright-and-monochromatic 7-eV laser-based light source and V-LEED detection system for resolving the spin polarizations of the photoelectrons. The use of the 7-eV probe is also advantageous for achieving a high momentum resolution, because the band structures in momentum (k) space are magnificently replicated in the angular distribution of the photoelectrons compared to the cases where probes of higher photon energies are adopted.

In the present project, we investigated the surface of a grey arsenic single crystal by using the laser SARPES apparatus. First, we found a pair of spin-polarized surface bands on the (111) face of grey arsenic (Figs. 1a and 1b). The pair forms two concentric Fermi surfaces

that enclose the surface Gamma point (Fig. 1c). The pair mimics the bands of two-dimensional free electrons subjected to the Rashba-type interaction. In fact, we observe that the bands show the expected polarization (Fig. 1d), and they can be nicely fit by the free electron bands subjected to the Rashba-type interaction (Fig. 1e): The best fit is obtained with the mass being 0.07 times that of a bare electron and the splitting of 0.0054 \AA^{-1} along k .

Combined with information of the band structures in the unoccupied side obtained by using time-resolved ARPES and the first principles calculation, we concluded that the spin-split surface bands discovered on As(111) occur due to reasons of the topology of the bulk band structure: That is, grey arsenic is a TI. Thus, we came to the picture that there is a boundary between phosphorous and arsenic in the group 15 elements, below which the elemental semimetals become topologically non-trivial. For further reading, see Ref. [6].

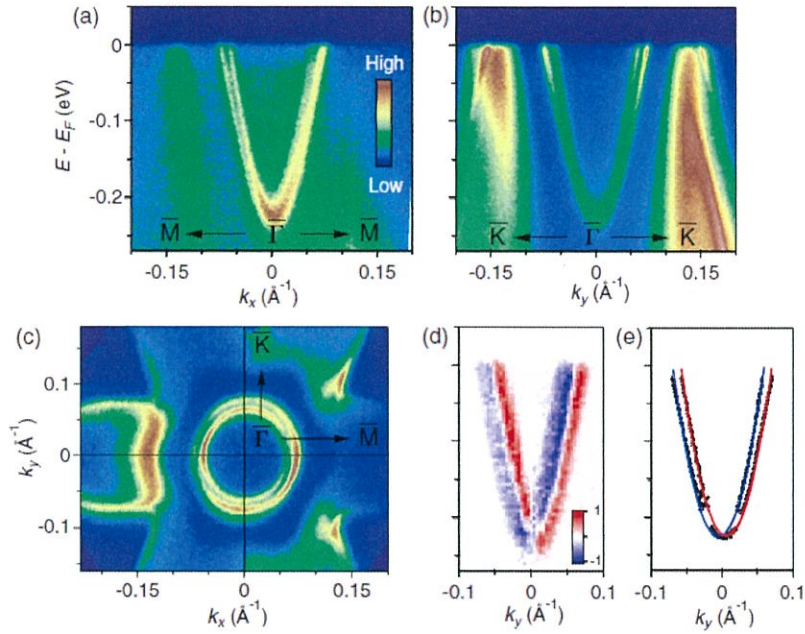


Fig. 1: Band structures of the 111 face of grey arsenic recorded by the laser SARPES apparatus. Band dispersions along k_x (a) and k_y (b). (c) Fermi surface mapping. (d) Spin polarization of the bands recorded by SARPES. (e) Fits of the dispersions to those of nearly-free electrons spin-split by the Rashba-type interactions.

REFERENCES

- [1] D. Hsieh, D. Qian, L. Wray, Y. Xia, Y. S. Hor, R. J. Cava, M. Z. Hasan, *Nature* **452**, 970 (2008).
- [2] Jimin Kim, Seung Su Baik, Sae Hee Ryu, Yeongsup Sohn, Soohyung Park, Byeong-Gyu Park, Jonathan Denlinger, Yeonjin Yi, Hyoung Joon Choi, Keun Su Kim, *Science* **349**, 723 (2015).
- [3] D. Hsieh, Y. Xia, L. Wray, D. Qian, A. Pal, J. H. Dil, J. Osterwalder, F. Meier, G. Bihlmayer, C. L. Kane, Y. S. Hor, R. J. Cava, M. Z. Hasan, *Science* **323**, 919 (2009).
- [4] Y. Ohtsubo, L. Perfetti, M. O. Goerbig, P. Le Fevre, F. Bertran, A. Taleb-Ibrahimi, *New J. Phys.* **15**, 033041 (2013); S. Ito, B. Feng, M. Arita, A. Takayama, R.-Y. Liu, T. Someya, W.-C. Chen, T. Iimori, H. Namatame, M. Taniguchi, C.-M. Cheng, S.-J. Tang, F. Komori, K. Kobayashi, T.-C. Chiang, and I. Matsuda, *Phys. Rev. Lett.* **117**, 236402 (2016).
- [5] K. Yaji, A. Harasawa, K. Kuroda, S. Toyohisa, M. Nakayama, Y. Ishida, A. Fukushima, S. Watanabe, C. Chen, F. Komori, S. Shin, *Rev. Sci. Instrum.* **87**, 053111 (2016).
- [6] P. Zhang, J.-Z. Ma, Y. Ishida, L.-X. Zhao, Q.-N. Xu, B.-Q. Lv, K. Yaji, G.-F. Chen, H.-M. Weng, X. Dai, Z. Fang, X.-Q. Chen, L. Fu, T. Qian, H. Ding, S. Shin, *Phys. Rev. Lett.* **118**, 046802 (2017).

LASER-SARPES STUDY ON THE INTERBAND HYBRIDIZATION OF SPIN-ORBIT COUPLED SURFACE STATES IN THIN FILMS

Ryo Noguchi¹, Kenta Kuroda¹, T. Kondo¹, M. Sakano¹, K. Yaji¹, A. Harasawa¹,
K. Kobayashi², F. Komori¹, and S. Shin¹

¹*The Institute for Solid State Physics, The University of Tokyo*

²*Department of Physics, Ochanomizu University*

Introduction:

The Rashba effect leads to spin-splitting in electronic structures at the surface or the interface of solids due to the broken inversion symmetry collaborated with spin-orbit coupling (SOC). In the conventional Rashba model, an eigenstate of the SO-induced spin-splitting is treated with an assumption of a fully spin-polarized state which protects electrons from backscattering. However, in real materials, the assumption can be usually broken because the SO coupling mixes different states with different orbitals and orthogonal spinors in a quasiparticle eigenstate. This SO entanglement can permit the spin-flip electron backscattering and moreover play a significant role in an emergence of the large spin-splitting. Therefore, it is essentially important to experimentally explore the SO coupling not only in the lifting spin degeneracy but also in the SO-entangled wavefunction as eigenstates.

Here, we report a direct investigation on the SO entanglement in the Rashba surface states of Bi/Ag(111) surface alloy by using a combination of polarization variable laser with spin- and angle-resolved photoemission spectroscopy (laser-SARPES). In contrast to the previous experiments [1, 2], our laser-SARPES deconvolves the orbital wavefunction and the coupled spin, and the surface wavefunctions are directly imaged into momentum-space through orbital-selection rule. It is shown that the interband SO coupling modifies the spin and orbital character of the surface states, leading to a large deviation from the conventional Rashba model [3].

Experimental:

Laser-SARPES was performed at newly home-built laser-SARPES machine at ISSP with high-flux 6.994-eV laser light. The laser-SARPES machine is based on two high efficient VLEED spin-polarimeters and the hemispherical analyzer with photoelectron deflector function (ScientaOmicron DA30L). This spectrometer can resolve spin polarization components of photoelectrons for in-plane ($P_{x,y}$) and out-of-plane (P_z) orientation. The spin polarized photoelectrons were excited by p - and s -polarized light (ε_p and ε_s , respectively). During the measurement, the sample temperature was kept around 15 K, and instrumental energy and angular resolutions were set below 20 meV and 0.7°, respectively [4].

Results:

A schematic of electronic structure of Bi/Ag(111) is shown in Fig. 1(a). The sp_z -derived bands and the higher-lying p_{xy} bands, dispersing downwards in energy with a large Rashba spin-splitting, are observed as shown in Fig. 1(b). Figure 1(c) summarizes the linear polarization dependence in Bi/Ag(111). Considering the orbital selection rule in the dipole excitation, ε_p selectively detects *even*-parity orbital with respect to the mirror plane, while ε_s is sensitive to the *odd*-parity orbital. For the result obtained by ε_p , we observe the strong intensity for the sp_z and inner p_{xy} bands [the left panel in Fig. 1(c)]. The data particularly displays the band crossing of the outer sp_z and inner p_{xy} bands around $k_x=0.15 \text{ \AA}^{-1}$, where the spectral intensity of the outer sp_z is strongly suppressed. Surprisingly, with the light polarization ε_s , the dispersion of the outer sp_z is clearly observed even at larger $k_x>0.15 \text{ \AA}^{-1}$ together with the outer p_{xy} band [the middle panel in Fig. 1(c)]. The right panel of Fig. 1(c) shows the differential intensity map. The

magenta-green colour contrast reflects the contribution of the *even*- and *odd*-orbital components in the surface wavefunction. It is immediately found that the orbital character of sp_z band changes the orbital character at the band crossing.

To get further insight into the influence of the interband SO coupling, we carried out laser-SARPES measurements collaborated with the orbital selection rule of ε_p and ε_s . Figure 1(d) shows spin-polarization and intensity maps obtained by ε_p and ε_s . For ε_p , the inner and outer sp_z -bands around $\bar{\Gamma}$ point in the both materials show negative and positive spin-polarization, respectively, displaying a conventional Rashba-type spin-texture. The observed spin polarization is found to be large up to nearly 80%. Most remarkably, we find that the sign of the spin polarization sensitively depends on the linear polarization. This can be seen particularly around $k_x=0.12 \text{ \AA}^{-1}$ in Bi/Ag(111). The spectral weight of the spin-up is considerably larger than the spin-down for ε_p and achieves nearly +80% spin-polarization. For ε_p , the intensity relation turns opposite and the resulting spin-polarization is found to be -70%. Since the linear polarization is sensitive to different orbital symmetry, our laser-SARPES unambiguously reveals that the spin direction strongly depends on the orbital character. We now show that the total spin information (P_{total}) can be traced back only by using a combination of the spin mapping with ε_p and ε_s lasers. Owing to selective detection of the pure orbital-symmetry in our experimental set-up, the orbital-dependence in the spin polarization is eliminated by integrations of spin-polarization maps [Fig. 1(e)] as follows:

$$P_{total} = \frac{(I_{\uparrow,p} + I_{\uparrow,s}) - (I_{\downarrow,p} + I_{\downarrow,s})}{(I_{\uparrow,p} + I_{\uparrow,s}) + (I_{\downarrow,p} + I_{\downarrow,s})}$$

where $(I_{\uparrow,p}, I_{\uparrow,s})$ and $(I_{\downarrow,p}, I_{\downarrow,s})$ are the spin-up and spin-down intensities obtained by $(\varepsilon_p, \varepsilon_s)$. The mapping of P_{total} clearly demonstrates the complex spin texture of the sp_z band under interband hybridization, which is comparable to the theoretical predictions. This technique demonstrates a general advantage to investigate the unconventional spin textures in strong SO-coupled states although the results could be influenced by the cross-section for ε_p and ε_s and the photoemission calculation to consider photon energy dependence is required.

REFERENCES

- [1] C. R. Ast, et al., Phys. Rev. Lett. **98**, 186807 (2007).
- [2] F. Meier *et al.*, Phys. Rev. B, **77**, 165431 (2008).
- [3] R. Noguchi *et al.*, Phys. Rev. B **95**, 41111 (2017).
- [4] K. Yaji *et al.*, Rev. Sci. Instrum., **87**, 053111 (2016).

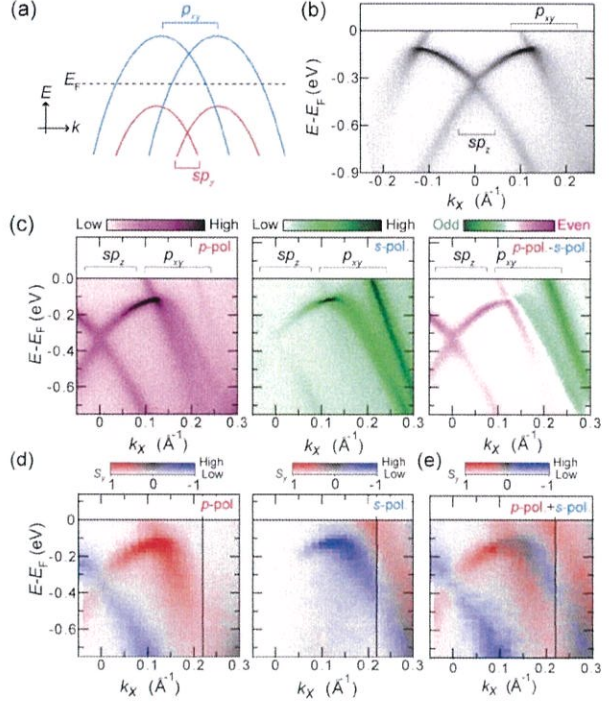


Fig. 1: (a) Schematic of the energy dispersion of Rashba spin-split bands in Bi/Ag(111). (b) ARPES intensity map with p -polarization along $\bar{\Gamma} - \bar{K}$ line of the surface Brillouin zone. (c) The magnified ARPES intensity maps with (left) p - and (middle) s -polarization, and (right) the differential intensity maps, which are obtained by $I_p - I_s$ where I_p and I_s are the photoelectron intensity obtained by p - and s -polarized light without intensity normalization. (d) Orbital-selective spin-polarization and photoelectron intensity maps obtained by (left) p - and (right) s -polarized light with the two-dimensional color codes. Spin quantum axis is set along y . (e) The total spin polarization (P_{total}) mapping.

MAPPING OF SPIN-ORBITAL ENTANGLEMENT IN THE NOVEL SUPERCONDUCTOR Sr_2RuO_4 BY USING LASER SPIN-RESOLVED ARPES

K. Kuroda¹, S. Akebi¹, M. Nakayama¹, M. Sakano, K. Yaji¹, A. Hasawa¹, H. Taniguchi²,
Y. Maeno², S. Nakatsuji¹, S. Shin¹ and T. Kondo¹

¹*The Institute for Solid State Physics, The University of Tokyo*

²*Department of Physics, Kyoto University*

Introduction:

Since the great discovery of superconductivity in Sr_2RuO_4 , many theoretical and experimental efforts have been paid for examining spin-triplet chiral p -wave superconductivity [1-3]. However, some recent experiments have not supported this, in which spin-triplet superconductivity alone was insufficient to explain the experimental facts [4, 5]. This contradiction mostly comes from the inclusion of low-energy fine-electronic structure and its wavefunction character due to spin-orbit coupling (SOC). It can be easily imagined that SOC can play a fundamental role beyond simple models for Cooper pairing mechanism, since the energy scale of the SOC of nearly 100 meV in Sr_2RuO_4 is much larger than the scale of $T_c \sim 0.2$ meV. In the presence of SOC, the quantum states with different orbitals and spins are generally mixed and the eigenstate wavefunction is strongly modified. This spin-orbital (SO) entanglement thereby results in the breakdown of singlets and triplets for Cooper pairing, although the both are generally used to treat novel superconductivity. Recently, the SO entanglement and its momentum dependence have been theoretically predicted in bulk Sr_2RuO_4 [6].

In this work, by using spin- and angle-resolved photoemission spectroscopy combined with 7-eV laser (Laser-SARPES), we have obtained the first experimental evidence of the SO entanglement in the eigenstate wavefunctions in Sr_2RuO_4 . We have recently shown that 7-eV excitation energy selectively detects the electronic structures at the top most (001) cleaved surface [7] and thereby the data we present here show the surface states. Our findings therefore hold importance not only for understanding mechanism of superconductivity but also possible topological edge states that might be detected below T_c on the side surfaces [8].

Experimental:

Laser-SARPES experiments were performed at newly home-built laser-SARPES machine at ISSP with high-flux 6.994-eV laser light [9]. The laser-SARPES machine is based on two high efficient VLEED spin-polarimeters and the hemispherical analyzer with photoelectron deflector function (ScientaOmicron DA30L). This spectrometer can resolve spin polarization components of photoelectrons in three-dimension for in-plane ($P_{x,y}$) and out-of-plane (P_z) orientation. The clean surface of Sr_2RuO_4 was *in situ* cleaved at below 20 K. During the measurement, the sample temperature was kept below 20 K, and instrumental energy and angular resolutions were set below 20 meV and 0.7° , respectively. All data was taken before sample degradation within 24 hours.

Results:

We start with a brief explanation for overall shape of Fermi surface obtained by our laser photon energy as shown in Fig. 1(a). The three-bands, α -band, γ -band and β -band, form the

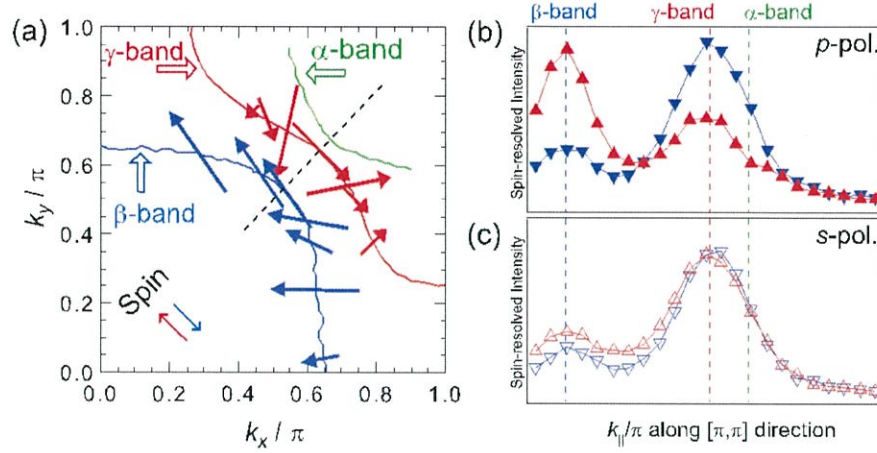


Fig. 1: (a) Shape of the Fermi surfaces for (001) cleaved surface state of Sr_2RuO_4 (open arrows, solid lines: α -, β - and γ -bands are shown green, red and blue lines, respectively). Our laser photon energy enables us to selectively detect only the surface signals [7]. (c) and (d) The spin-resolved momentum-distribution curves (MDCs) by using p - and s -polarization set up, respectively. These MDCs are obtained at k_{\parallel} cut along (π, π) direction as denoted by dashed line in Fig. 1(a). The red and blue triangles respectively show the spin-up and spin-down states, and the resolved spin axis is perpendicular to the momentum cut [see the inset in Fig. 1(a)]. The obtained momentum dependence of the spin direction and its size is shown by closed arrows in Fig. 1(a).

Fermi surface indicated by open arrows (α -, β - and γ -bands are shown green, red and blue lines, respectively). We observe clear the evidence of the SOC along (π, π) k_{\parallel} direction [dashed line in Fig. 1(a)], where these three bands are located close to each other. Figures 1(b) and (c) present spin-resolved momentum-distribution curves along this k_{\parallel} cut [the resolved spin axis is shown in the inset of Fig. 1(a)]. We clearly observe the large photoelectron spin-polarization for β - and γ -bands for p -polarization [Fig. 1(b)]. This photoelectron spin-polarization is shown to be originated from the photoemission matrix element effect, since the large spin-polarization is absent in the both bands for s -polarization [Fig. 1(c)]. Interestingly, we find clear k_{\parallel} dependence [see closed arrows in Fig. 1(a)]. Most remarkably, the direction of the photoelectron spin-polarizations is always opposite for β - and γ -bands [*e.x.* see Figs. 1(a)]. Moreover, it is worth noting that the orientation is insensitive to the experimental geometry. These results strongly indicate that the observed spin-polarization and its k_{\parallel} dependence present the SO entanglement in initial state wavefunctions.

References:

- [1] K. Ishida *et al.*, Nature **396**, 658 (1998).
- [2] T. M. Riseman *et al.*, Nature **396**, 242 (1998).
- [3] K. D. Nelson *et al.*, Science **306**, 1151 (2004).
- [4] S. Kittaka *et al.*, Phys. Rev. B **80**, 174514 (2009).
- [5] S. Yonezawa *et al.*, Phys. Rev. Lett. **110**, 077003 (2013).
- [6] C. N. Veenstra *et al.*, Phys. Rev. Lett. **112**, 127002 (2014).
- [7] T. Kondo *et al.*, Phys. Rev. Lett. **117**, 247001 (2016).
- [8] S. Kashiwaya *et al.*, Phys. Rev. Lett. **107**, 077003 (2011).
- [9] K. Yaji *et al.*, Rev. Sci. Instrum., **87**, 053111 (2016).

ELECTRONIC STATES AND ELECTRON-PHONON COUPLING IN 1D NANORIPPLED GRAPHENE ON MACROFACET OF 6H-SiC

Fumio Komori^{1,*}, Koichiro Ienaga¹, Takushi Iimori¹, Koichiro Yaji¹, Toshio Miyamachi¹,
Shuhei Nakashima¹, Yukio Takahashi¹, Kohei Fukuma², Shingo Hayashi², Takashi Kajiwar²,
Anton Visikovskiy², Kazuhiko Mase^{3,4}, Kan Nakatsuji⁵, and Satoru Tanaka²

¹*Institute for Solid State Physics, The University of Tokyo, 5-1-5 Kashiwanoha, Kashiwa,
Chiba 277-8581, Japan*

²*Department of Applied Quantum Physics and Nuclear Engineering, Kyushu University,
Fukuoka 819-0395, Japan*

³*Institute of Materials Structure Science, High Energy Accelerator Research Organization,
Tsukuba 305-0801, Japan*

⁴*Department of Materials Structure Science, SOKENDAI (The Graduate University for
Advanced Studies), 1-1 Oho, Tsukuba 305-0801, Japan*

⁵*Department of Materials Science and Engineering, Tokyo Institute of Technology,
Yokohama 226-8502, Japan*

Modulation of the graphene electronic states by one-dimensionally (1D) periodic potential at a nanoscale has been theoretical predicted, such as an energy gap at the Dirac point and anisotropic dispersion relation [1]. We prepared a nano-rippled graphene on a vicinal SiC(0001) substrate, and measured its band structure by angle resolved photoelectron spectroscopy (ARPES). For the same sample, the interaction between Dirac electrons and phonon system was studied using inelastic scanning tunneling spectroscopy (IESTS). We found spatially-dependent inelastic tunneling with the period of the nano-ripple structure. This clarified the structure of nano-rippled graphene used in this research. [2]

The ARPES measurement was carried out using the ARPES spectrometers with a He discharge tube at Kashiwa, ISSP, and with linearly-polarized light of 49 eV in BL13B of Photon Factory at KEK. Besides ARPES measurements, IESTS at 80 K were performed at ISSP. The nano-rippled graphene was fabricated by thermal decomposition of a SiC (0001) substrate with a slope of 4° in an Ar atmosphere. The graphene that was carried in the atmosphere to the ARPES chambers was annealed in an ultrahigh vacuum for the cleaning the surface before the measurements.

Figure 1 shows the STM image and the LEED image. As shown in Fig. 1 (a), the surface consists of terrace and macrofacets of 27°. A part of the terrace consists of graphene as shown in Fig. 1 (b) and so called a buffer layer with a $6\sqrt{3} \times 6\sqrt{3}$ superstructure. In the macrofacet part, graphene with one-dimensional undulation in the facet direction can be seen. In the

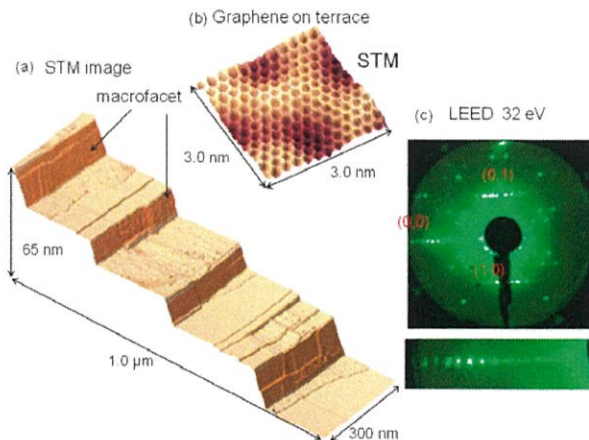


Fig. 1 STM images (a,b) and LEED pattern (c) of the sample surface. A repeated macrofacet and terrace structure is formed on the substrate as in (a). One-dimensionally nano-rippled structure can be seen on the macrofacet surface. On a part of the terrace, single-layer graphene with surface modulation due to the buffer layer at the subsurface was formed as in (b). In LEED pattern, (c), satellite graphene spots due to the nano-rippled graphene structure appear around the integer spots of graphene on the macrofacets. Magnified image of the satellite spots is shown in the lower part in (c).

LEED image, satellite spots were observed, reflecting of the undulated macrofacet as shown in Fig. 1 (c). The enlarged STM image of the macrofacet part is shown in Fig. 2. There is a periodic undulation on the macrofacet with graphene atomic structure, which indicates continuous graphene covering the macrofacet. The modulation period is 3.4 nm, which is coincident with the period obtained from the satellite spot interval of the LEED image shown in Fig. 1 (c).

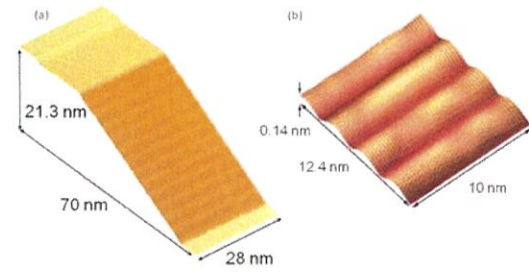


Fig. 2 Magnified STM images including a macrofacet (a) and with atomic resolution (b).

Figure 3 shows the ARPES image of the Dirac band from this facet. As shown in Fig. 3 (a) at 21.2 eV, satellite band signals were observed reflecting the one-dimensional super periodicity of the graphene on the macrofacet. The Dirac point of this graphene is 0.8 eV below Fermi energy, and the amount of doping is smaller than that of the graphene on the terrace. A band gap was not clearly observed, and the electron velocity was not significantly different from that on the terrace. When measured at 40.8 eV, signals from the second-layer graphene were also clearly observed as shown in Fig. 3 (b).

Furthermore, in the STS measurement, we observed inelastic tunneling signals due to phonons in the vertical direction of the graphene plane. This signal intensity periodically oscillates in the 1D undulation direction of graphene. This means that the intensity of the inelastic scattering due to the electron-phonon interaction oscillates in the tilting direction of the macrofacet. Since the STM image of the graphene surface looked uniform, we concluded that the intensity oscillation is attributed to the second layer graphene under the surface.

As a result, we propose a structural model of the graphene shown in Fig. 4. There are graphene nanoribbons and buffer layers at the interface with the SiC substrate. The tunneling electrons are easy to move from the surface graphene to the second layer nanoribbon in the former part, but in the latter, electrons are difficult to move because of the long interlayer distance. Due to this difference, the probability that tunnel electrons interact with the phonon system is larger in the latter.

In conclusion, one-dimensional nano-rippled graphene was fabricated on macrofacet of 6H-SiC substrate. Graphene Dirac band was confirmed by ARPES measurement. We proposed a structural model of this graphene by ARPES and STM / STS measurements.

REFERENCES

- [1] C.-H. Kim *et al.*, *Nature Phys.* **4**, 213 (2008).
- [2] K. Ienaga *et al.*, *Nano. Lett.* **17**, 3527 (2017).

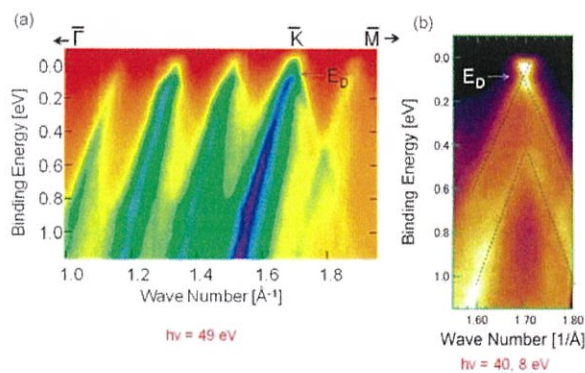


Fig. 3 ARPES spectra using 49 eV (a) and 40.8 eV (b).

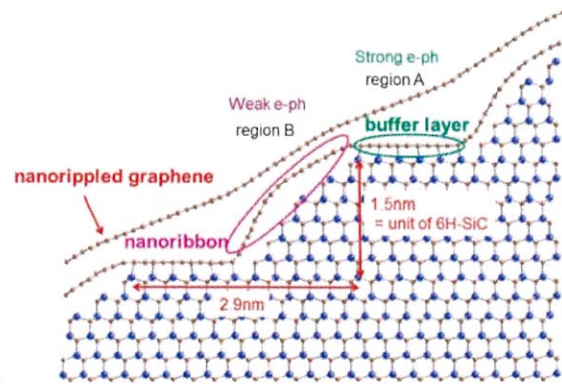


Fig. 4 A proposed model of the graphene on the macrofacet.